PARAMETRIZATION, ALIGNMENT AND SHAPE OF SPHERICAL SURFACES

Xiuwen Liu, John Bowers

Department of Computer Science, Florida State University, Tallahassee, FL, 32306, USA

Washington Mio

Department of Mathematics, Florida State University, Tallahassee, FL, 32306, USA

Keywords: Surface parametrization, surface alignment, shape geodesics, shape of surfaces, shape metric, texture maps.

Abstract: We develop parametrization and alignment techniques for shapes of spherical surfaces in 3D space with the goals of quantifying shape similarities and dissimilarities and modeling shape variations observed within a class of objects. The parametrization techniques are refinements of methods due to Praun and Hoppe and yield parametric mesh representations of spherical surfaces. The main new element is an automated technique to align parametric meshes for shape interpolation and comparison. We sample aligned surfaces at the vertices of a dense common mesh structure to obtain a representation of the shapes as organized point-clouds. We apply Kendall's shape theory to these dense point clouds to define geodesic shape distance, to obtain geodesic interpolations, and to study statistical properties of shapes that are relevant to problems in computer vision. Applications to the construction of compatible texture maps for a family of surfaces are also discussed.

1 INTRODUCTION

The representation and analysis of 3D geometric structures are fundamental problems in areas such as computer vision and medical imaging. The practical relevance of these problems is increasing vertically in tandem with the fast evolution of scanning technologies that allow us to acquire geometric structural data both at the macroscopic and microscopic levels. The geometry of the outer contour of an object is of particular interest as it carries a rich amount of 3D visual information that can enable us to classify and discern objects, analyze patterns of variation, and model the temporal evolution of their shapes in the presence of dynamics. In this paper, we develop techniques for constructing parametrizations and for aligning closed surfaces of genus zero, which are presented as meshes in 3D Euclidean space $\mathbb{R}^3$. An example of a closed surface of genus zero – that is, a surface that can be obtained as a deformation of a round sphere – is shown in Figure 1. We apply the parametrization and alignment methods to the following problems: (i) the construction of compatible low-distortion meshes for a family of surfaces; (ii) the interpolation of spherical shapes; (iii) the development of metrics to quantify shape similarity and dissimilarity; (iv) the construction of compatible texture maps for a family of shapes; (v) the calculation of mean shapes. These problems are all relevant to computer vision as they arise in the modeling of variations in shape and appearance, for example, in 3D object recognition.

Unlike a curve that has a natural parametrization by the arc-length parameter, no such special parametrization exists for a surface. As a consequence, discrete models of surfaces used in practice often adopt representations involving highly non-uniform samplings, especially for surfaces whose geometry exhibit thin and elongated parts, high curvature areas, or other sharp features. Meshes representing such surfaces tend to exhibit many regions that are either undersampled or oversampled and contain many triangles with undesirable aspect ratios. To address these issues, parametrizations of spherical surfaces by mappings that minimize the average geometric distortion have been investigated in (Praun and Hoppe, 2003). Let $\mathbb{S}^2$ denote the unit sphere centered at the origin in $\mathbb{R}^3$ and let $\phi \colon \mathbb{S}^2 \to M$ be a parametrization of a spherical surface M embedded in $\mathbb{R}^3$. The infinitesimal distortion produced by the mapping ϕ at $x \in \mathbb{S}^2$ was quantified by the sum of
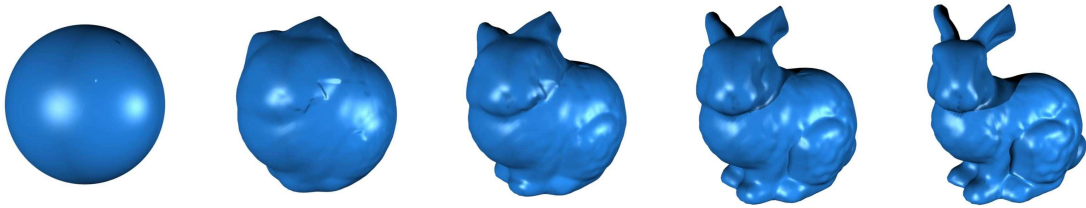
Figure 1: The contour of a bunny as a deformation of a round sphere.

the squares of the singular values of the derivative $d\phi(x)$, the linearization of ϕ at x. However, this measure of distortion is heavily biased towards stretching and only mildly penalizes compression. This has the practical effect of controlling undersampling of the parametrizations – but not oversampling – and allowing the parametrizations to distort aspect ratios in a significant way. A solution to this problem was proposed in (Praun and Hoppe, 2003), but the cost function utilized is highly asymmetric with respect to stretching and compression. In this paper, our contribution to the construction of spherical parametrizations is a refinement of the model of Praun and Hoppe based on a fully symmetric measurement of distortion that leads to more uniform meshes. The process of remeshing a surface with this technique to improve regularity is illustrated in Figure 3. From a more technical perspective, we also introduce some alternative computational strategies for the implementation of the parametrization algorithm.

The main new element of this paper is an algorithm to align parametric surfaces of genus zero in a fully automated manner. Alignment is of basic importance in shape interpolation and in the development of shape metrics. Without alignment, interpolations tend to be intuitively incorrect (Alexa, 2000). In several previous works on shape interpolation, such as (Alexa, 2000) and (Asirvatham et al., 2005), alignment is done with the aid of manually chosen landmark points. Here, alignment is based on an optimal matching of the outward unit normal fields to the surfaces, which capture important geometric properties to first order. Applied to a family of spherical surfaces, the parametrizaton and alignment methods allow us to obtain compatible parametrizations for the family that, on average, optimally match corresponding features and minimize metric distortions. Once such family of parametrizations has been constructed, one can remesh the given surfaces using a common reference spherical triangulation of $\mathbb{S}^2$ and use these meshes for multiple purposes such as interpolating shapes, defining shape metrics, studying the statistics of shapes, and applying texture maps to the entire family in a compatible fashion.

The paper is organized as follows. In Section 2, we describe an algorithmic procedure to construct "regular" parametrizations of surfaces of genus zero. Sections 3 and 4 are devoted to the problem of aligning surfaces. A brief review of Kendall's shape model is presented in Section 5.1, which is followed by applications to shapes of surfaces. Mean shapes are discussed in Section 6, as an introduction to the statistical study of shapes of surfaces.

2 PARAMETRIZATIONS

Let a closed surface of genus zero in $\mathbb{R}^3$ be presented as a mesh M. A spherical parametrization of M consists of a spherical triangulation K of the sphere $\mathbb{S}^2$ together with an embedding $\phi\colon \mathbb{S}^2 \to M \subseteq \mathbb{R}^3$ such that ϕ respects the mesh structures. Thus, vertices, edges (that is, great circles connecting adjacent vertices) and spherical triangles of K are mapped to the corresponding structures in M. To construct parametrizations, we normalize M by scaling it to have a fixed total area, say, 4π.

For each $x \in M$, let $J_{\phi^{-1}}(x)$ denote the Jacobian of the inverse map $\phi^{-1}\colon M \to \mathbb{S}^2$ at x, and let $0 < \gamma(x) \leq \Gamma(x)$ be the singular values of $J_{\phi^{-1}}(x)$. In (Praun and Hoppe, 2003), the metric distortion of ϕ is quantified by the average value of

$$\frac{1}{\gamma^2(x)} + \frac{1}{\Gamma^2(x)} \tag{1}$$

over M. If $p = \phi^{-1}(x) \in \mathbb{S}^2$, then the singular values of $J_\phi(p)$ are $1/\gamma(x)$ and $1/\Gamma(x)$. Thus, (1) is heavily biased toward stretching due to ϕ, since sizable stretching corresponds to small values of γ, while high compression relates to large values of Γ. To address this issue, a term proportional to the sixth power of Γ is added to (1), but the proposed solution is rather ad hoc and highly asymmetric with respect to stretching and compression. We modify the cost function to the average value of

$$\log^2 \gamma(x) + \log^2 \Gamma(x), \tag{2}$$

which is perfectly symmetric in that stretching and compression by the same factor are penalized identically. Note that, on a logarithmic scale, the magnitude of the singular values of $J_{\phi^{-1}}(x)$ and $J_\phi(p)$ are the same. Moreover, (2) vanishes precisely in the case where both singular values are 1; that is, if there is no infinitesimal distortion at x.

To estimate the cost function, Praun and Hoppe subdivide the mesh K until each triangle is "sufficiently" planar and approximate each spherical triangle τ in the subdivided mesh by the planar triangle $\tau_1 \subset \mathbb{R}^3$ spanned by its vertices. Let T be a triangle in the associated subdivision of M that corresponds to τ via ϕ. Then, ϕ^{-1} is approximated by the linear map $A_T: T \to \tau_1$ determined by the vertex correspondence. The singular values of $J_{\phi^{-1}}(p)$ are approximated by the singular values of A_T over the triangle T, for any $x \in T$. However, if the triangles have bad aspect ratio, large errors may occur in the estimation of the singular values even after taking fine subdivisions of K. To cope with this problem, they precede the subdivision of K with another subdivision step that attempts to improve aspect ratios. We adopt a different approach to a reliable estimation of the singular values. We replace the linear approximation to each spherical triangle with the planar triangle obtained via the exponential map, as described next. Let v be the vertex of τ determined by its two longest sides of length ℓ_1 and ℓ_2, respectively, and let θ be the internal angle at v. We approximate τ with the plane triangle τ_2 determined by ℓ_1, ℓ_2 and θ, as indicated in Figure 2. Note that τ_2 is well defined up to rigid motions, which will not affect singular values. The advantage of τ_2 is that, for small triangles, it gives a better approximation of the geometry of τ even for nearly degenerate triangles. As before, the singular values are estimated using the linear map $T \to \tau_2$ determined by the vertex correspondence.

Figure 2: A spherical triangle flattened via the exponential map.

Praun and Hoppe employ a coarse-to-fine strategy – analogous to that adopted in (Hormann et al., 1999) and (Sander et al., 2002) – to construct a spherical embedding that parameterizes M. The mesh M is decimated sequentially until it is reduced to a tetrahedron. This gives a multiresolution representation of M as a sequence of meshes. A spherical parametrization that minimizes the cost function is first constructed at the coarse tetrahedral level and then progressively refined through the various intermediate levels to a

parametrization of M with minimal distortion. We refer the reader to (Praun and Hoppe, 2003) for further details. Figures 3 (a) and (b) show a mesh on a bunny and the result of remeshing the shape by transferring a regular mesh on the sphere via a minimal distortion parametrization, respectively. A close-up view is shown on panels (c) and (d). Note that the triangles are much more regular in the remeshed surface.
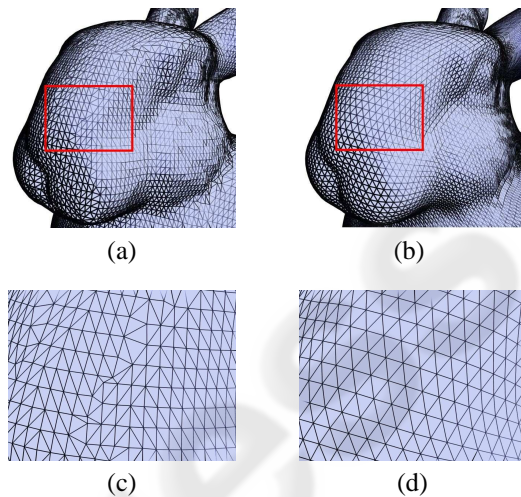

Figure 3: Remeshing the surface of a bunny: (a) the original mesh; (b) transferring a regular spherical mesh from $\mathbb{S}^2$ with a minimal-distortion parametrization; (c) and (d) are close-up views.

Similar to (Gu et al., 2002), minimal-distortion parametrizations can be used to transfer texture patterns from the sphere $\mathbb{S}^2$ to a shape as illustrated in Figure 4.

3 SHAPE ALIGNMENT

Let M_1 and M_2 be meshes in 3D space representing spherical surfaces. Using the procedure described in Section 2, construct parametrizations $\phi^i: \mathbb{S}^2 \to M_i$, for $i = 1, 2$. Before aligning the shapes, we remesh them with respect to a fixed triangulation K of $\mathbb{S}^2$, typically chosen to have fairly uniform triangles. Then, each ϕ^i can be viewed as a mapping $K \to M_i$ that respects the mesh structures. The idea is to consider reparametrizations of one the shapes to best match the geometry of the other using the alignment of the outward unit normal fields as criterion. We first discuss reparametrizations.

Given a parametric shape $\phi: \mathbb{S}^2 \to M$ and a rotation matrix $R \in SO(3)$, we consider reparametrizations of M of the form

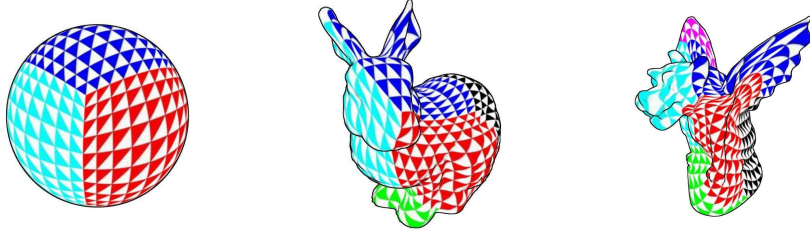$$p \mapsto \phi(R^T p), \tag{3}$$

Figure 4: Transferring texture from a sphere to a shape with a minimal-distortion parametrization.

which simply rotates the sphere $\mathbb{S}^2$ before mapping it to M via ϕ. We denote this new parametrization of M by ϕ_R. Note that the singular values of $J_\phi^{-1}(x)$ and $J_{\phi_R}^{-1}(x)$ are the same, for any $x \in M$. Thus, if ϕ is a minimal distortion parametrization, as measured by (2), then ϕ_R is also minimal.

Given a rotation matrix R and a pair of parametrizations ϕ^1 and ϕ_R^2, for each $p \in \mathbb{S}^2$, we think of $\phi^1(p) \in M_1$ and $\phi_R^2(p) \in M_2$ as corresponding points and wish to measure the average discrepancy of the normal fields $N_1(p)$ and $N_2(p;R)$, for $p \in \mathbb{S}^2$. Normal fields are insensitive to translations and scale, but they do change under rotations and reflections of a surface. Thus, before comparing the normal fields of ϕ_1 and ϕ_R^2, we find the orthogonal matrix $U \in O(3)$ that minimizes

$$\iint_{\mathbb{S}^2} \|N_1(p) - U\left(N_2(p;R)\right)\|^2 \, dp. \qquad (4)$$

In practice, the most interesting triangulations K of $\mathbb{S}^2$ are those that are fairly dense and uniform. For these, the minimizer of (4) can be estimated as

$$U_R = \underset{U \in O(3)}{\operatorname{argmin}} \sum_{v \in K} \|N_1(v) - U\left(N_2(v;R)\right)\|^2, \qquad (5)$$

where the sum is taken over the vertices v of K. The solution to (5) can be computed in closed form, as follows. Order the vertices of K as $v_1, \ldots, v_\ell$ and form the $3 \times \ell$ matrices P and Q_R, whose jth columns are the normal vectors $N_1(v_j)$ and $N_2(v_j;R)$, respectively. Let the singular value decomposition of PQ_R^T be given by

$$PQ_R^T = U\Sigma W^T, \qquad (6)$$

with $V, W \in O(3)$ and Σ diagonal with nonnegative eigenvalues. Then,

$$U_R = UW^T. \qquad (7)$$

The reparametrization of ϕ^2 that best aligns the parametric shapes $\phi^1, \phi^2 \colon K \to \mathbb{S}^2$ is determined by the rotation matrix

$$\hat{R} = \underset{R \in SO(3)}{\operatorname{argmin}} H(R), \qquad (8)$$

where

$$H(R) = \iint_{\mathbb{S}^2} \|N_1(p) - U_R\left(N_2(p;R)\right)\|^2 \, dp. \qquad (9)$$

4 ALIGNMENT ALGORITHM

The alignment of M_1 and M_2 is implemented in two stages: first, we carry out a coarse estimation of $\hat{R}$ by sampling the functional H over a large finite set of rotations. Subsequently, a local refinement is performed using a gradient search. An alternative stochastic gradient procedure will be discussed elsewhere.

4.1 Coarse Estimation

Let $\eta_1, \ldots, \eta_s$ be a fairly uniformly distributed and dense collection of unit vectors to be thought of as determining axis of rotations of $\mathbb{R}^3$. An example of such a set is the collection of vertices of the triangulation K of $\mathbb{S}^2$ used in the previous section. Divide the interval $[0, 2\pi]$ uniformly into r parts to obtain angles $0 = \theta_0 < \theta_1 < \ldots < \theta_r = 2\pi$. We sample H over the set $R(\eta_i, \theta_j)$, $1 \leqslant i \leqslant s$, $1 \leqslant j \leqslant r$, of rotations about the axis η_i by the angle θ_j. As in (5), for a rotation R, the calculation of the functional H uses the following discretization over the vertices of the mesh K:

$$H(R) = \sum_{v \in K} \|N_1(v) - U_R\left(N_2(v;R)\right)\|^2. \qquad (10)$$

The top results are recorded and a finer search is carried out around each of these candidates.

4.2 Local Refinement

The space $SO(3)$ of 3×3 rotation matrices R is a 3-dimensional manifold (as a matter of fact, a Lie group). To perform the aforementioned gradient search, we first describe the tangent space to $SO(3)$ at R. Let

$$E_1 = \begin{bmatrix} 0 & 1 & 0 \\ -1 & 0 & 0 \\ 0 & 0 & 0 \end{bmatrix}, \quad E_2 = \begin{bmatrix} 0 & 0 & 0 \\ 0 & 0 & 1 \\ 0 & -1 & 0 \end{bmatrix},$$
$$E_3 = \begin{bmatrix} 0 & 0 & 1 \\ 0 & 0 & 0 \\ -1 & 0 & 0 \end{bmatrix}. \qquad (11)$$

For any $R \in SO(3)$, the matrices

$$E_i^R = \frac{1}{\sqrt{2}} R E_i, \qquad (12)$$

$1 \leqslant i \leqslant 3$, form an orthonormal basis of the tangent space to $SO(3)$ at R. A geodesic deformation of R along the direction E_i^R is given by

$$R_i(t) = R e^{t E_i / \sqrt{2}}. \qquad (13)$$

We estimate the partial derivatives of H in the directions E_i^R, as follows:

$$\partial_i H(R) \approx \frac{H(R_i(\varepsilon)) - H(R)}{\varepsilon}, \qquad (14)$$

with $\varepsilon > 0$ small. The gradient of H at R can be calculated as

$$\nabla H(R) = R A_R, \qquad (15)$$

where $A_R = \sum_{i=1}^{3} \frac{\partial_i H(R)}{\sqrt{2}} E_i$. The (geodesic) update rule for the gradient search is

$$R_{j+1} = R_j e^{-\delta A_{R_j}}, \qquad (16)$$

with $\delta > 0$ small.

5 SHAPE OF SURFACES

We employ the parametrization and alignment techniques presented in Sections 2 and 3 to model and quantify shape similarity and divergence within a given collection of spherical meshes $M_1, \ldots, M_k$. First, construct minimal distortion parametrizations $\phi_i \colon \mathbb{S}^2 \to M_i$, $1 \leqslant i \leqslant k$. Choose a spherical triangulation K of $\mathbb{S}^2$, which will be used to align and discretize the parametrizations. Remesh all surfaces with respect to K using the parametrizations ϕ_i – we abuse terminology and still refer to the new meshes as M_i. Each ϕ_i can now be viewed as a mesh-preserving mapping $K \to M_i$. To simplify the discussion, we align each ϕ_j, $2 \leqslant j \leqslant k$, with respect to ϕ_1. This type of alignment will be biased toward the first shape, so refinements of the alignment will be discussed below. An advantage of remeshing all surfaces over K is that the alignment of the surfaces induce a natural correspondence between the vertices of any pair M_i and M_j, $i \neq j$. We exploit this fact to study the shapes of the surfaces.

We order the vertices of K arbitrarily as $v_1, \ldots, v_n$ and discretize each M_i using the ordered point cloud $\phi_i(v_1), \ldots, \phi_i(v_n)$. Since correspondences have been established between the point clouds associated to any pair of surfaces, we can resort to Kendall's shape theory to analyze the shapes of the surfaces (Kendall, 1984), (Kendall et al., 1999). We briefly review the model, which uses a Procrustean alignment of shapes and a geodesic metric to quantify shape divergence.

5.1 Kendall's Model

For a parametric shape $\phi \colon K \to M$, we write the coordinate vectors of the vertices $\phi(v_1), \ldots, \phi(v_n)$ as the columns of a $3 \times n$ matrix P. Ordered configurations of vertices that differ by rigid motions or scale are to be viewed as having the same shape. To eliminate translational effects from the representation, the ordered point cloud is translated to have its centroid at the origin. This amounts to subtracting the mean

$$\mu_\phi = \frac{\phi(v_1) + \ldots + \phi(v_n)}{n} \in \mathbb{R}^3 \qquad (17)$$

from each column of the matrix P. To fix the scale, a centered matrix P is normalized to have Frobenius norm 1. Centered matrices of unit norm are referred to as pre-shapes. Heretofore, we assume that all matrices have been normalized to represent pre-shapes.

Unlike translation and scale, there is no standard normalization that satisfactorily accounts for rotations and reflections. This is due to the facts that rotational alignment for shape comparison depends on the shapes that are being compared in a more essential manner and the relevance of chirality tends to be contextual. Given pre-shapes P, Q, the best alignment in Kendall's model is given by the orthogonal matrix $\hat{U} \in O(3)$ characterized by

$$\hat{U} = \underset{U \in O(3)}{\operatorname{argmin}} \| P - UQ \|^2. \qquad (18)$$

$\hat{U}$ is the orthogonal transformation that places Q closest to P as measured by the Frobenius norm. Using a singular value decomposition, write $PQ^T = V_1 \Sigma V_2^T$, with $V_1, V_2 \in O(3)$ and Σ diagonal with nonnegative eigenvalues. Then, $\hat{U} = V_1 V_2^T$. The shape distance is the geodesic distance between the pre-shapes P and $\hat{Q} = \hat{U} Q$, which can be expressed as

$$d(P, Q) = \arccos(\operatorname{tr} \Sigma). \qquad (19)$$

Moreover, if $P \neq \hat{Q}$, the geodesic deformation between P and $\hat{Q}$ is given by

$$\Lambda(t) = \cos(\omega t) P + \sin(\omega t) \frac{\hat{Q} - (\operatorname{tr} \Sigma) P}{\| \hat{Q} - (\operatorname{tr} \Sigma) P \|}, \qquad (20)$$

where $\omega = \arccos(\operatorname{tr} \Sigma)$ and $0 \leq t \leq 1$.

5.2 Algorithm

The following algorithmic steps compute the Kendall geodesic between the shapes represented by the pre-shapes P and Q:

1. Find a singular value decomposition $PQ^T = V_1 \Sigma V_2^T$.

2. Set $\hat{Q} = V_1 V_2^T Q$.

3. If $P = \hat{Q}$, the geodesic is represented by the constant path $\Lambda(t) = P$. Else, it is given by (20).
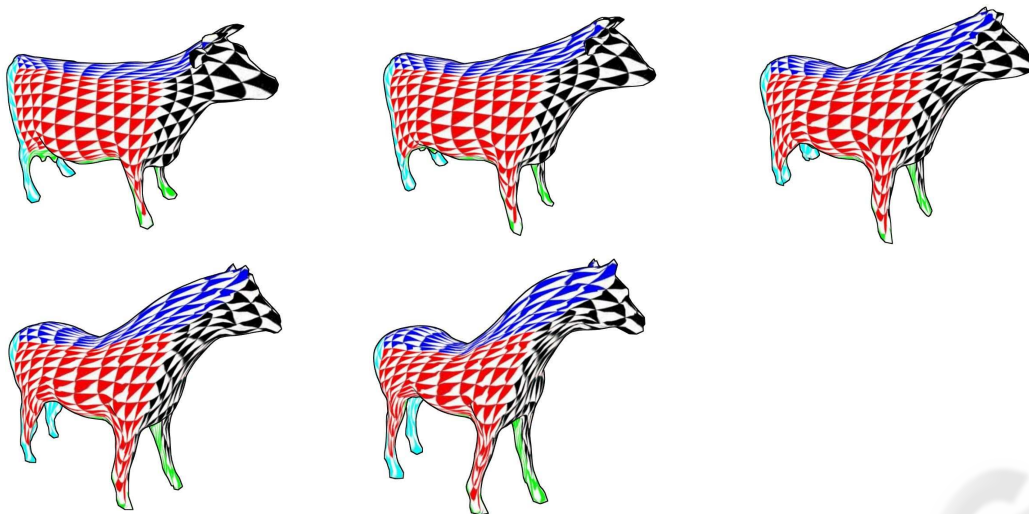
Figure 5: A shape geodesic with a compatible texture map applied to the deformation.

5.3 Examples of Geodesics

An example of a geodesic interpolation between a horse and a cow is shown in Figure 5. To calculate the geodesic, we first remesh the shapes to be interpolated over a common spherical triangulation K of $\mathbb{S}^2$ and align them using the algorithm of Section 4. Subsequently, the point clouds given by the vertices of the meshes are interpolated using Kendall's model. The point-cloud interpolation between the (ordered) vertex sets is displayed in Figures 6 (a)–(e). At any stage of the interpolation, the vertices of K are in correspondence with the point cloud. Thus, the mesh structure on K can used at all stages of the geodesic path to obtain meshes as indicated in the last row of Figure 6. As exemplified in Figure 5, these aligned spherical parametrizations allows us to apply texture maps to the entire path in a compatible manner.

6 FRÉCHET MEAN SHAPES

To illustrate the usefulness of the algorithm for calculating shape geodesics in the study of shape statistics, we indicate how one can define the notion of mean shape using a natural extension of Fréchet means in Kendall's theory (Kendall et al., 1999). If $s_1, \ldots, s_r$ are spherical shapes, a mean shape will be defined as follows. First, parameterize all shapes over a common spherical mesh K and align them all with respect to, say, the first one. This fixes a parametrization for each of the shapes. Let $P_1, \ldots, P_r$ be the pre-shapes associated with the vertices of the meshes induced by these parametrizations over K. Then, a mean of the family is a shape represented by a pre-shape P that minimizes the scatter function

$$V(P) = \frac{1}{2} \sum_{i=1}^{r} d^2(P, P_i). \qquad (21)$$

Techniques for calculating the mean in Kendall's theory are discussed, e.g., in (Karcher, 1977). Figure 9 shows the mean of 4 horses. As well documented in the literature, in other contexts, once the sample mean of a collection has been computed, one can estimate probability models for the family using the exponential map at the mean and tangent-space statistics (Dryden and Mardia, 1998).

7 SUMMARY AND CONCLUSION

We developed techniques to produce parametric representations $\phi \colon \mathbb{S}^2 \to M$ of spherical surfaces that refine the methods of (Praun and Hoppe, 2003). The parametrizations are constructed so as to minimize the overall distortion in geometry. A method for aligning parametric surfaces to best match their unit normal fields was introduced. The procedure is fully automated and can be used to quantify shape similarity and divergence, and to model shape variations observed within a class of objects. In conjunction with Kendall's shape theory, the alignment technique yields a metric for shape comparison and geodesic shape morphing technique. Applications to the construction of compatible texture maps for a family of surfaces and the calculation of mean shapes were discussed.
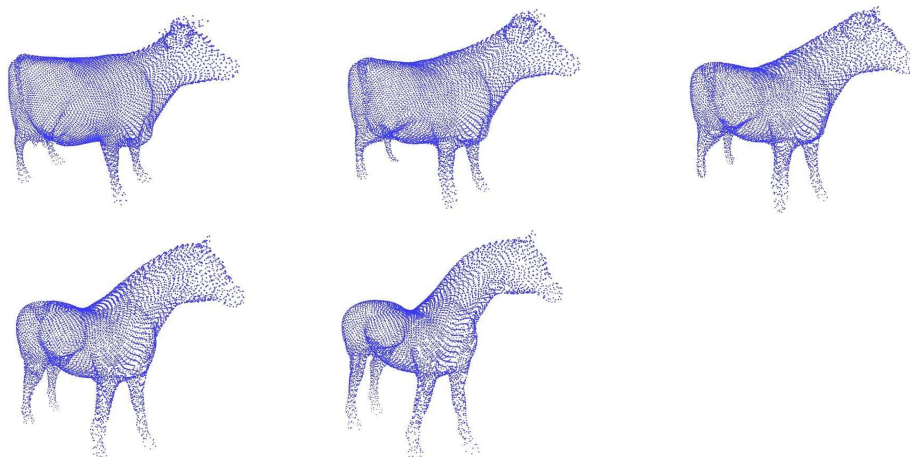
Figure 6: A geodesic interpolation between ordered point clouds. The first and last frames display the shapes to be interpolated and the intermediate frames show 3 stages of the deformation.
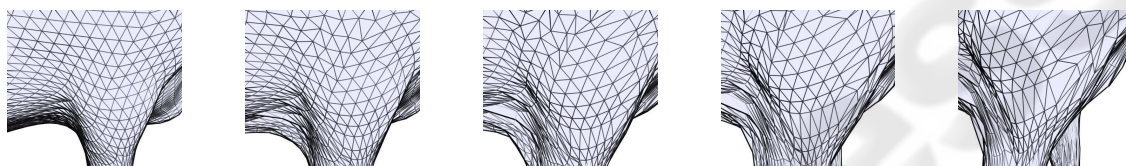

Figure 7: Close-up view of the evolution of the mesh structure associated with the point clouds in Figure 6.

Alignment of shapes is based on reparametrizations of a shape by rotations of the sphere $\mathbb{S}^2$. This is natural in the proposed setting since the action of rotations preserve the minimal-distortion property of a parametrization. In future work, the alignment technique will be refined to an elastic alignment to better match the geometric features of the surfaces. The Kendall model of shapes was applied to a dense point cloud representing a surface. While this is already very useful and attractive from a computational standpoint due to the simplicity of the model, the shape metric fails to incorporate important higher order surface geometry. The shape metric and interpolation technique will also be refined to a model that can be computed efficiently and which takes higher order geometry into account.

ACKNOWLEDGMENTS

REFERENCES

Alexa, M. (2000). Merging polyhedral shapes with scattered features. *The Visual Computer*, 16(1):26–37.

Asirvatham, A., Praun, E., and Hoppe, H. (2005). Consistent spherical parametrization. In *Workshop on Computer Graphics and Geometric Modeling (CGGM)*.

Dryden, I. L. and Mardia, K. V. (1998). *Statistical Shape Analysis*. John Wiley & Son.

Gu, X., Gortler, S., and Hoppe, H. (2002). Geometry images. In *ACM SIGGRAPH 2002*, pages 355–361.

Hormann, K., Greiner, G., and Campagna, S. (1999). Hierarchical parametrization of triangulated surfaces. In *Vision, Modeling, and Visualization*, pages 219–226.

Karcher, H. (1977). Riemann center of mass and mollifier smoothing. *Comm. Pure Appl. Math.*, 30:509–541.

Kendall, D. G. (1984). Shape manifolds, Procrustean metrics and complex projective spaces. *Bull. London Math. Soc.*, 16:81–121.

Kendall, D. G., Barden, D., Carne, T. K., and Le, H. (1999). *Shape and Shape Theory*. Wiley, Chichester, New York.

Praun, E. and Hoppe, H. (2003). Spherical parametrization and remeshing. In *ACM SIGGRAPH 2003*, pages 340–349.

Sander, P., Gortler, S., Snyder, S., and Hoppe, H. (2002). Signal-specialized parametrization. In *Eurographics Workshop on Rendering*, pages 87–100.
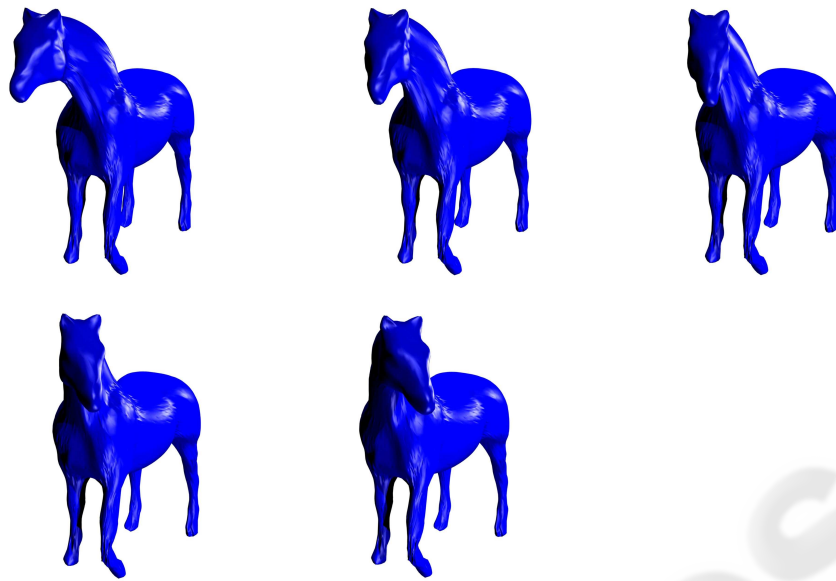
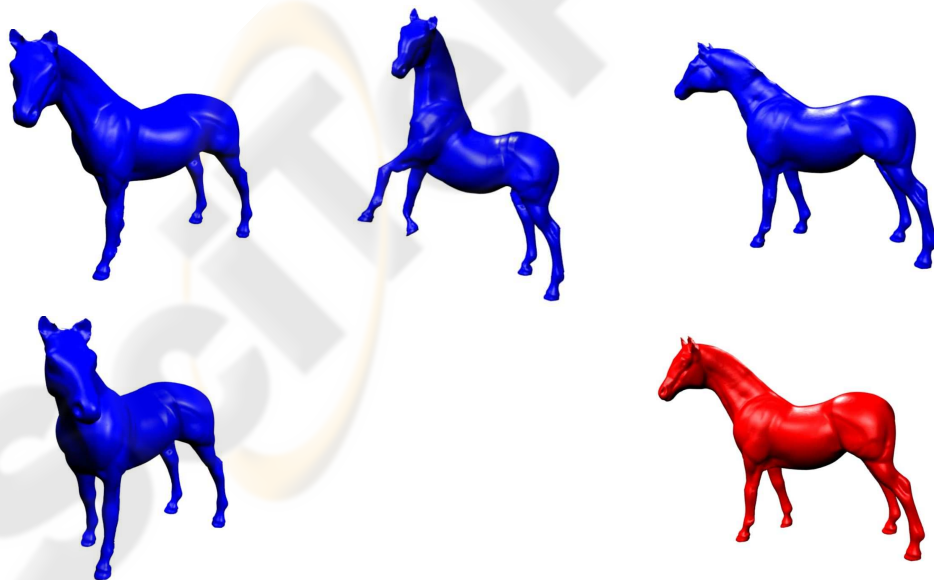Figure 8: An example of a shape geodesic morphing a horse into another horse.

Figure 9: Four horses and their Fréchet mean shape, which is shown on the bottom-right panel.